Nucleic Acids Research, 2000, Vol. 28, No. 13 **2455–2461**

RNA accessibility prediction: a theoretical approach is consistent with experimental studies in cell extracts

Michaela Scherr[1,2], John J. Rossi[2], Georg Sczakiel[3,4] and Volker Patzel[3,*]

[1]Abteilung für Hämatologie und Onkologie, Medizinische Hochschule Hannover, Carl-Neuberg-Strasse 1, D-30625 Hannover, Germany, [2]Department of Molecular Biology, Beckman Research Institute, City of Hope, 1450 East Duarte Road, Duarte, CA 91010-3011, USA, [3]Deutsches Krebsforschungszentrum, F0200, Im Neuenheimer Feld 242, D-69120 Heidelberg, Germany and [4]Medizinische Universität zu Lübeck, Institut für Molekulare Medizin, Ratzeburger Allee 160, D-23538 Lübeck, Germany

Received as resubmission April 30, 2000; Accepted May 11, 2000

ABSTRACT

The use of antisense oligodeoxyribonucleotides (ODN) or ribozymes to specifically suppress gene expression is simple in concept and relies on efficient binding of the antisense strand to the target RNA. Although the identification of target sites accessible to base pairing is gradually being overcome by different techniques, it remains a major problem in the antisense and ribozyme approaches. In this study we have investigated the potential of a recent experimental and theoretical approach to predict the local accessibility of murine DNA-methyltransferase (MTase) mRNA in a comparative way. The accessibility of the native target RNA was probed with antisense ODN in cellular extracts. The results strongly correlated with the theoretically predicted target accessibility. This work suggests an effective two-step procedure for predicting RNA accessibility: first, computer-aided selection of ODN binding sites defined by an accessibility score followed by a more detailed experimental procedure to derive information about target accessibility at the single nucleotide level.

INTRODUCTION

Sequence-specific inhibition of gene expression by antisense nucleic acids and ribozymes is a rapidly growing area with increasing impact on molecular medicine and gene function analysis (1–7). The basic principle underlying these strategies is that efficient annealing of complementary sequences to the target RNA can elicit enzymatic, site-specific destruction of this RNA. Theoretically, any sub-sequence of the target RNA can be chosen as a site for antisense binding. Experience tells one, however, that the extent of gene suppression can differ widely with the choice of the target site. This is due to differing local target accessibilities which are a consequence of complex secondary and tertiary intramolecular folding. For long chain antisense RNAs and ribozymes, effective annealing to the target is further dependent upon the structure of the antisense strand (8). Conversely, short antisense oligodeoxyribonucleotides (ODN) have a restricted potential to form stable intramolecular structures and their efficacy is strongly dependent on local target accessibility. In two seperate studies only 1 of 20 ODN tested showed significant (>50%) inhibition of target gene expression (9,10). Thus, it has been a fundamental goal of antisense investigators to develop techniques to identify accessible local target sites. So far, a variety of *in vitro* techniques have been developed to predict the accessibility of a chosen mRNA (11–17). Many of these are combinatorial approaches based on annealing reactions with arrays of antisense species (see for example ref. 13) and/or monitoring accessibility of target structures by *Escherichia coli* RNase H mapping (see for example 12,15).

In the living cell, however, RNA structure and, thus, accessibility are thought to be dependent on the intracellular environment. Annealing reactions and duplex stability of complementary nucleic acids are known to be influenced by RNA-binding proteins (18–21). Further, cellular RNase H might reveal properties distinct from the bacterial enzyme used in experimental mapping. Thus, a system has recently been developed to detect the accessibility of ODN binding to native target RNA via cleavage by endogenous, cellular RNase H in cell extracts (11). Although this method allows the evaluation of target accessibility under conditions closely related to the intracellular environment, it is affected by experimental limitations which cannot be excluded or controlled. Theoretical approaches, such as computational target screening, bypass experimental limitations but are restricted in their resolution of target accessibility and depend on the reliability of structure prediction. We recently described a computer-aided, semi-empirical procedure to substantially increase the statistical probability of identifying local target sites accessible to antisense ODN (22). This theoretical approach makes use of a systematic alignment of computer-predicted secondary structures of local sequence stretches (windows) of the target RNA and takes into consideration several minimum free energy structures.

In this study we have compared the potential of the accessibility predictions using antisense ODN in cellular extracts (11) with the theoretical approach (22). As a target sequence we chose the mRNA encoding murine DNA-methyltransferase (MTase; EMBL accession no. X14805). MTase-dependent DNA methylation plays an important role in regulating biological functions such as gene expression and cellular differentiation (23). The MTase mRNA is GC-rich (60–70%) and, therefore, highly

*To whom correspondence should be addressed. Tel: +49 6221 424938; Fax: +49 6221 424932; Email: patzel@dkfz-heidelberg.de

structured, which makes it difficult to identify accessible sites for base pairing with antisense ODN or ribozymes. The results of this study demonstrate a strong correlation between the data obtained by probing the native RNA with ODN in cellular extracts or in living cells and the theoretically predicted target accessibility. Under the conditions used, the theoretically derived data only partially corresponded to those obtained from a non-cell extract assay using *E.coli* RNase H activity (11). This work suggests the use of combined computational and experimental methods to predict RNA accessibility for maximizing antisense ODN and ribozyme binding.

MATERIALS AND METHODS

Oligodeoxyribonucleotides

The phosphodiester and phosphorothioate ODN were prepared in the DNA synthesis facility of the City of Hope (Duarte, CA). The anti-MTase ODN used in this study were as follows (5′→3′): sense control, d(GCAAACAGAAATAAAAAGCCA); scrambled control, d(TCGTGCCCACGGGTCATGTTGT); as1041, d(CCAGTTTTTTACGTGTCG); as860, d(AAGTGAGTTTCCGGTCTTGC); as863, d(TCCAAGTGAGTTTCCGGTCT); as855, d(TTTCCGGTCTTGCTTCTC); as867, d(CGTCCAAGTGAGTTTCCG); as4300, d(CCCTGAGGATGGGCTGGTAG); as4303, d(GGTCCCTGAGGATGGGCTGG); as4304, d(GTCCCTGAGGATGGGCTG). The ODN used in cell extracts had two terminal internucleotide phosphorothioates at both the 5′- and 3′-ends.

The synthetic ODN MT1-5′, d(GCTGGGTCCGGAAGAGCCATGTG), and MT1-3′, d(CTTCTCAATGAGACCGGTGTC), were used for RT–PCR amplification of MTase mRNA from position 761 to 1381. The ODN MT3-5′, d(TCAGGAACTTCGTGTCCTACAG), and MT3-3′, d(GGGCACCGGTGCTGCTGTAGCC), were used to amplify by RT–PCR the mRNA from position 3890 to 4502. The ODN MT1-3′ and MT3-3′ were 5′-end-labeled with hexachloro-6-carboxyfluorescein (HEX) and the 3′-β-actin ODN (internal control) was 5′-end-labeled with 6-carboxyfluorescein (FAM).

Preparation of cellular extracts and RT–PCR

The cellular extracts used in these studies were always freshly prepared from 3×10^7 NIH 3T3 cells as described previously (11). The ODN RNA mapping experiments were carried out in 20 µl of freshly prepared cellular extract containing 40 U RNase inhibitor (Promega, Madison, WI) and 50 nM of each antisense ODN. Incubation of the ODN was for 2–15 min at 37°C, after which the mixture was treated with DNase I and extracted with phenol–chloroform. Reverse transcription followed by DNA PCR was performed as described previously (11). The murine housekeeping gene β-actin served as an internal standard and as a loading control. The resulting amplicons were monitored and quantified on an Applied Biosciences Prism 377 DNA Sequencer using GeneScan analysis software v.2.1 (ABI, Weiterstadt, Germany). As a size marker, the GeneScan-2500 TAMARA standard with molecular lengths (bp) 827, 536, 490, 470, 361, 269, 238, 233, 222, 186, 172, 116, 109, 94 and 37 was used.

Computer-aided RNA accessibility prediction

The computer-aided RNA accessibility prediction was performed as described previously (22).

RESULTS AND DISCUSSION

Definition of an accessibility score for local target sequences

The formation of the first 2–3 bp (nucleation event) leading to a base-specific complex between two complementary strands is assumed to be the rate limiting step of duplex formation (24), which may be followed by a faster cooperative zippering mechanism leading to the double-stranded product (24,25). It is reasonable to assume that unpaired nucleotides of a target RNA are involved in the nucleation event. When considering the higher thermodynamic stability of intramolecular RNA–RNA duplexes over RNA–DNA heteroduplexes, it seems to be easier for an antisense ODN to invade and pair with a target structure if open structural target motifs exceed the size required for nucleation.

The theoretical approach described recently to identify accessible local target sites is based on a systematic alignment of computer-predicted secondary structures of overlapping sequence stretches (windows) of the target RNA (22). Schematically, the target RNA is broken down to windows of a given size W_{size} (here 1400 nt), the sequence stretch corresponding to the first window is folded by the mfold program (v.2.0), the five lowest free energy structures (s1–s5) are aligned and the window is shifted by a step width W_{width} (here 500 nt). After analysis of the last window, the structures of overlapping windows are aligned. Local target sites were proposed to be accessible to antisense ODN if they were composed of large (≥10 nt) consecutive sequence stretches not involved in base pairing, such as loops, bulges, joint sequences or free ends. In order to identify such favorable motifs with a high statistical probability of success only those motifs were selected by the algorithm which were conserved among a variety of sequence windows and conserved among several minimum free energy structures for each window. However, this procedure is qualitative in nature and does not allow scoring and comparison of the accessibility of local target sites. In order to achieve this goal, we defined an accessibility score $SC_{acc}(i)$ for individual local target motifs i (equation **1**):

$$SC_{acc}(i) = [S_i \times P_i \times (W_{s1,i})/100]/(W_{seq,i} + W_{tot}) \quad \mathbf{1}$$

where S_i is the average size in nucleotides of favorably predicted local target motifs, P_i is the probability score reflecting the impact of favorably predicted local target motifs within a target structure analysis, $W_{s1,i}$ is the portion (%) of analyzed windows with a lowest free energy structure s1 containing a favorable local target motif, $W_{seq,i}$ is the number of windows containing a sequence stretch (≥10 nt) which folds within one or more s1 structures into a favorable motif and W_{tot} is the total number of analyzed sequence windows. This score transforms the qualitative data obtained by the computational structure alignment into a quantifiable form and enables quantitative comparison of experimental and theoretical RNA accessibility predictions.

Equation **1** was derived empirically on the basis of the experimental data obtained for *ICAM-1* mRNA (22). S_i is the average number of nucleotides contained in favorably

predicted target motifs (≥10 consecutive unpaired nucleotides) of the lowest free energy structures s1 of each analyzed sequence window. For example, target t860 (Fig. 1B) appears in windows w1 and w2. The s1 structures of w1 and w2 contain favorable target motifs of 17 and 13 nt in length, respectively, resulting in $S_{(t860)} = 15$. In case of target t1041 only the s1 structure of w2 contains a favorable target motif of 11 nt in length. Thus $S_{(t1041)} = 11$. P_i is a parameter which reflects the fact that different minimum free energy structures have, according to their energy levels, different impacts on target structure analysis. Empirically, 20 points were assigned to the appearence of a favorable target motif (only motifs with ≥10 contiguous unpaired nucleotides were assumed to be favorable) within the lowest free energy structure (s1) of each window, 10 points for its appearance within the second lowest (s2), 5 for the third lowest (s3), 2 for the fourth lowest (s4) and 1 for the fifth lowest (s5) free energy structure (mfold v.2.0). Other ratings of the different low energy structures or the use of the more recent mfold v.2.3 did not give satisfactory results. P_i reflects the sum of all points given to a favorable target motif within a complete target analysis, including all structures (s1–s5) of all analyzed windows. Therefore, P_i is a direct function of the total number of analyzed windows W_{tot}. The term including W_{tot} in the denominator of equation **1** partly compensates for this dependence. $W_{seq,i}$ reflects the number of windows containing a sequence stretch (≥10 nt) which folds within one or more s1 structures into a favorable motif. As a result of consecutively shifting a window with a defined step width along a target sequence, centrally located sequences are analyzed in more windows compared to sequences in the proximity of either the 5′- or 3′-end and, thus, could create a stronger P_i compared to promising terminally located target sites. To avoid an underestimation of such target sites, $W_{seq,i}$ is added to W_{tot}. $W_{s1,i}$ (%) is the portion of analyzed windows with a lowest free energy structure s1 containing a local target sequence which folds into a favorable local target motif. For example, in the case of targets t860 and t4300 the s1 structures (Fig. 1B and D) of all analyzed windows covering these target sites contain a consecutive stretch of ≥10 unpaired nucleotides and, thus, $W_{s1(t860)}$ and $W_{s1(t4300)}$ are 100% (Table 2). Conversely, target t1041 appears in three (w1–w3) of nine (w1–w9) analyzed windows but only the s1 structure of window 2 (w2) contains a favorable structure element at this site. For this reason $W_{s1(t1041)}$ corresponds to 33% (Table 2).

So far, the accessibility score defined here does not distinguish between different classes of favorable target motifs, such as loops, bulges, joints and free ends. To investigate these differences in a statistically solid fashion, additional experimental data will be required.

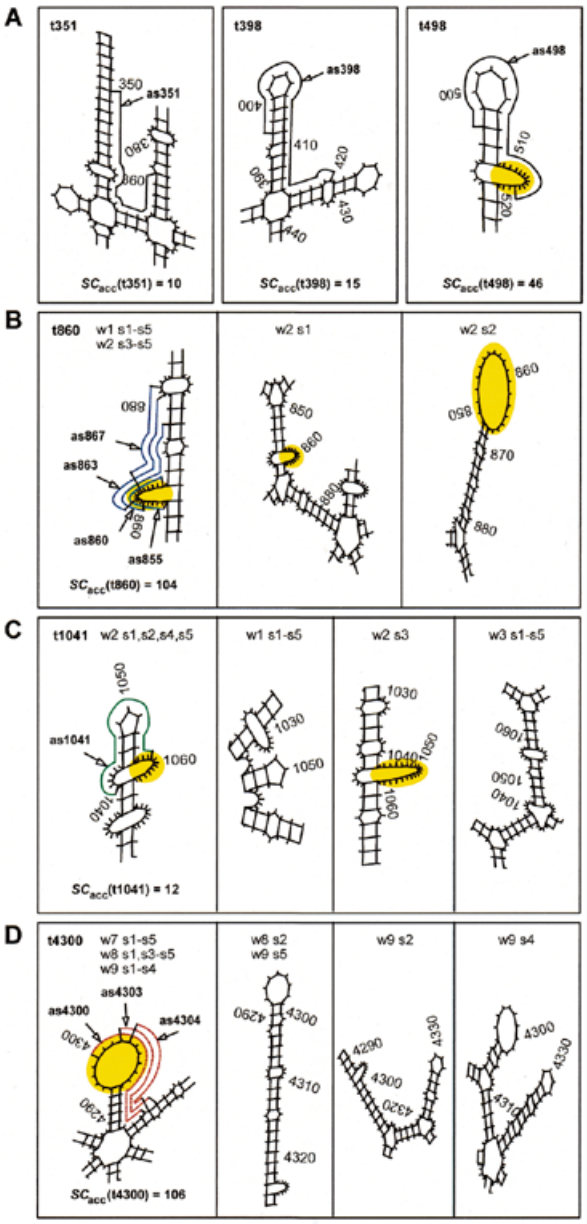

Figure 1. Predicted secondary structures of local targets of the MTase mRNA. Accessibility scores SC_{acc}(i) and binding sites of tested antisense ODN are indicated. (**A**) Lowest free energy structures of target sites analyzed by Scherr and Rossi: t351 (left), t398 (middle) and t498 (right). (**B**–**D**) Target sites identified by the computational analysis of the full-length mRNA. t860 (B) and t4300 (D) are favorable targets, while t1041 (C) is a less favorable target according to SC_{acc}(i). The lowest free energy structures (s1–s5) of local targets for all analyzed windows (w1–w9) are indicated. Blue, t860-directed antisense ODN; green, t1041-directed antisense ODN; red, t4300-directed antisense ODN; yellow, favorable (≥10 contiguous unpaired nucleotides) target motifs.

Experimental versus theoretical RNA accessibility prediction

In this work we have investigated and compared a theoretical (22) and a recent experimental (11) approach to identify and evaluate local structures of RNA that are accessible for annealing with antisense ODN. The experimental approach in this comparison is based on binding of antisense ODN to native mRNA in cell extracts followed by cleavage with endogenous RNase H and quantification by RT–PCR of the remaining, uncleaved target using fluorescence tagged primers and GeneScan analysis. Both methods were used independently to analyze the accessibility of the murine MTase mRNA for three antisense ODN, as351, as398 and as498 (11).

As reported recently (11), ODN as498 was most effective in cell extracts, reducing the MTase mRNA levels to 15%,

followed by as398 (50%) and as351 (80%) (Table 1). The data derived from experiments with cell extracts corresponded well with the efficacy in living cells and to a lower extent with the *in vitro* antisense ODN-directed *E.coli* RNase H mapping of *in vitro* transcribed substrate (Table 1; 11). However, the varying extent of reduction in MTase mRNA by the antisense ODN did not correlate with the secondary structure prediction of the corresponding target sites based on the mfold program (11). On the other hand, when computational target screening was applied, significant differences in target accessibilities were predicted for the three local target sites (Fig. 1A). An accessibility score of SC_{acc}(t498) = 46 was calculated for the target of ODN as498, t498, which was predicted to contain a bulge of 13 nt (Fig. 1A, right). For target t398, which corresponds to ODN as398, a significantly lower accessibility score of SC_{acc}(t398) = 15 was calculated (Fig. 1A, middle). Target t351, containing a perfect stem of 13 nt in length, seemed to be inaccessible, with a calculated SC_{acc}(t351) value of 10 (Fig. 1A, left).

Table 1. Relationship between the computer-predicted RNA accessibility of the MTase mRNA and the activity of antisense ODN *in vitro*, in cell extracts and in living cells

Antisense ODN[a]	Accessibility score	*In vitro* assay[a,b] (%)	Assay using cellular extracts[a] (%)	*In vivo* assay[a] (%)
as351	10	20	80 ± 5	100
as398	15	15	50 ± 6	73 ± 3
as498	46	8 ± 3	15 ± 10	18 ± 4

[a]Sequences and data are described in Scherr and Rossi (11). % designates the percentage in MTase mRNA relative to the control sense and scrambled ODN.
[b]The *in vitro* assay was performed using 1 nM substrate and 10 nM antisense ODN.

SC_{acc}(i) is a statistical parameter reflecting the probability of a local target site being accessible to an antisense ODN. Thus, a high accessibility score should always be related to high antisense ODN-mediated cleavage by RHase H in the experimental assays, such as observed for targets t860 and t4300. Conversely, not all local targets found in the experimental assays to be accessible to antisense ODN can be expected to be related to a high SC_{acc}(i) value. For example, such a target is t498. This target seems to be as accessible to antisense ODN as targets t860 and t4300 (Table 1 and Fig. 3), despite a significantly lower accessibility score, which is the consequence of lower structural conservation. If, depending on the analyzed sequence window, favorable and unfavorable local structures are predicted for a single target site, the computational analysis results in an intermediate accessibility score, although the 'real' RNA structure might be either highly accessible or inaccessible.

For the three analyzed target sites, the theoretically derived ranking of the local target accessibilities seems to correspond better with the data derived in cell extracts and in living cells than with the *E.coli* RNase H mapping of the *in vitro* transcribed substrate (Table 1). This might be due to the fact that the ratio of antisense ODN to target RNA was too high, allowing detection of a wider range of differences in accessibility in the *in vitro* assay.

Both strategies, experimental RNase H mapping of endogenous transcripts and computer-based theoretical target screening, seem to be suitable techniques to predict *in vivo* active antisense ODN. A major advantage of the theoretical approach is that it is not restricted by the length of the analyzed target sequence. Furthermore, it can be directly used for target screening to identify the most favorable target sites.

Computational accessibilty scanning of the complete murine MTase mRNA

A major advantage of the theoretical approach is that it bypasses all experimental limitations, including limitations concerning the length of the target to be screened for accessible sites. In order to test this potential we computationally reinvestigated the complete MTase mRNA. No highly favorable target was located within the first 600 5′ nucleotides analyzed previously by the experimental procedure. Two favorable targets, t860 [SC_{acc}(t860) = 104; Fig. 1B] and t4300 [SC_{acc}(t4300) = 106; Fig. 1D], as well as the less favorable target t1041 [SC_{acc}(t1041) = 12; Fig. 1C], were tested experimentally with regard to their effectiveness (Figs 2 and 3). All parameters which are relevant for calculation of the SC_{acc} values are listed in Table 2. Four t860-directed antisense ODN (as855, as860, as863 and as867), three t4300-directed ODN (as4300, as4303 and as4304) and the t1041-directed ODN (as1041) were tested for reduction of MTase mRNA in cellular extracts. It seems that t4300 is more accessible to antisense ODN pairing than t860. The t4300-directed antisense ODN (red bars) showed an average mRNA reduction to 12% and the t860-directed antisense ODN (blue bars) to 22% (Fig. 3). Target t1041 seems to be less accessible compared to either of the other target sites. These data are signifcantly correlated with the computational accessibility predictions (Table 2). For both selected favorable targets, t860 and t4300, antisense ODN reduced MTase mRNA levels in the experimental assay under standard conditions to the maximally reduced levels described in the literature so far (11).

One has to address the question of whether the SC_{acc}(i) values depend on the window size and on the step width used. The data in Table 3 indicate that for a given step width of 500 nt a reduction in the window size from 1400 to 700 nt results in values of SC_{acc}(i) which are no longer compatible with the experimental accessibility mapping of the MTase mRNA. This result indicates that a sequence context of the target RNA of 700 nt might not be sufficient for reliable secondary structure prediction of local sites within a long mRNA target sequence. For example, one might assume that independent structural folding units are frequently disrupted in the case of too small window sizes. In another calculation, for a given window size of 1400 nt, the step width was modified. In principle, the lower the step width the higher the resolution of the analysis. A reduction of W_{width} from 1000 to 500 and 250 nt indicated that SC_{acc}(i) values were similar at $W_{width} \leq 500$ nt (Table 3). An exception is SC_{acc}(t1041). In terms of predicted accessibility, the structure of the local target t1041 is only poorly conserved among different foldings and strongly depends on the sequence context (Fig. 1C). Together these

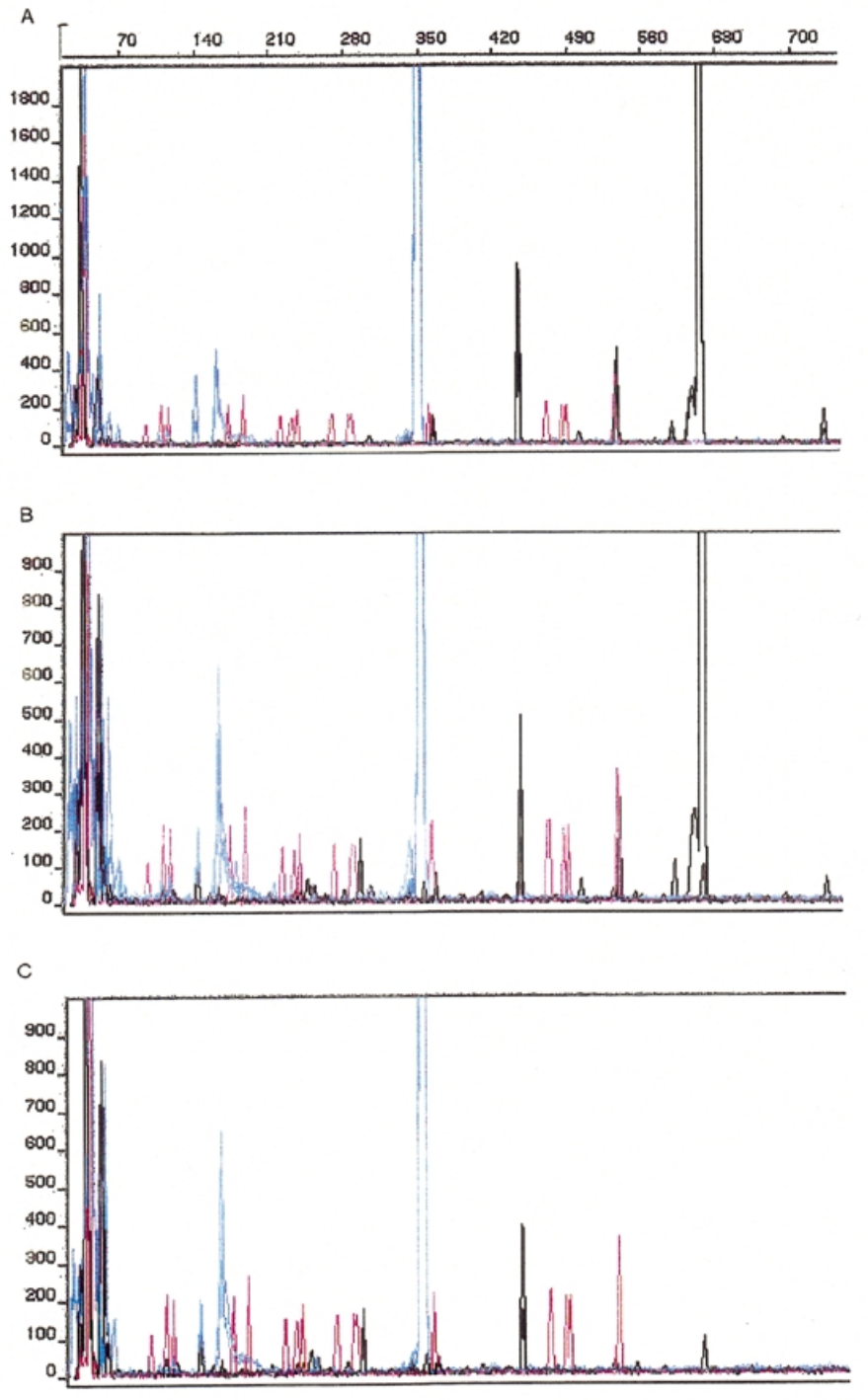

Figure 2. GeneScan analysis of RNase H-mediated cleavage of endogenous mRNA in cell extracts using anti-MTase ODN. The relative signal strength is plotted versus the length of the PCR fragments. (**A**) RT–PCR followed by DNA PCR was performed with control ODN-treated cellular extract. The PCR fragments are of the expected size of ~620 bp for MTase (black peak), as depicted at the top, and 350 bp for β-actin (blue peak). (**B**) Cellular extract treated with the ODN as1041. RT–PCR followed by DNA PCR and GeneScan analysis was performed. The black peak (620 bp) shows the remaining MTase amplicon. (**C**) Cellular extract treated with the ODN as855. RT–PCR followed by DNA PCR and GeneScan analysis was performed. A small black peak corresponding to the 620 bp long MTase amplicon was observed. The red peaks are the TAMARA standards as described in Materials and Methods.

results indicate that a maximum step width of 500 nt and a window size of 1400 nt are suitable in order to obtain reproducible $SC_{acc}(i)$ values which are in significant agreement with experimental accessibility screening.

Table 2. Parameters for the calculation of SC_{acc} of the targets t860, t1041 and t4300

Target	$SC_{acc}(i)$	S_i	P_i	Structures[a]	$W_{s1,i}$ (%)	$W_{seq,i}$	Window (target position)	W_{tot}
t860	104	15	76	s1–s5	100	2	w1 (1–1400)	9
				s1–s5			w2 (501–1900)	
t1041	12	11	38	–	33	3	w1 (1–1400)	9
				s1–s5			w2 (501–1900)	
				–			w3 (1001–2400)	
t4300	106	14	91	s1–s5	100	3	w7 (3001–4400)	9
				s1,s3–s5			w8 (3501–4900)	
				s1,s3			w9 (3868–5267)	

[a]Low energy structures containing ≥10 consecutive unpaired nucleotides.

Table 3. Relationship between SC_{acc} values of different local targets, the step width W_{width} of the analyzed windows and the window size W_{size}

Target	W_{width} = 1000 nt W_{size} = 1400 nt	W_{width} = 500 nt W_{size} = 1400 nt	W_{width} = 250 nt W_{size} = 1400 nt	W_{width} = 500 nt W_{size} = 700 nt
t351	17	10	10	11
t398	25	15	17	15
t498	76	46	46	43
t860	107	104	106	65
t1041	76	12	44	76
t4300	126	106	110	35

According to the length of the target RNA, a step width of 1000, 500 or 250 nt corresponds to 5, 9 or 16 analyzed windows, respectively.

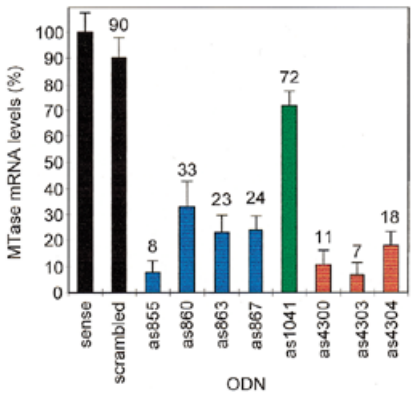

Figure 3. Levels of murine DNA methyltransferase mRNA in cellular extracts in the presence of antisense ODN. A sense ODN (100% MTase PCR product) and a scrambled ODN served as controls. The bars represent average values of three independent measurements and the degrees of deviation are indicated. Black, controls; blue, t860-directed antisense ODN; green, t1041-directed antisense ODN; red, t4300-directed antisense ODN.

A protocol for the selection of effective antisense ODN target sequences

The computational target screening substantially increases the probability of successful selection of antisense ODN that are effective in living cells. The accessibility score is a useful measure to compare and to select target sites by computational target screening, especially for long target sequences for which a large number of promising targets may exist. In sum, this work suggests an effective protocol for the selection of biologically active antisense ODN which consists of two steps: first, computer-aided selection of the most favorable local target sites using the accessibility score $SC_{acc}(i)$ and, second, a more focused experimental procedure to identify the most effective antisense ODN positioned within the predicted most accessible target sites. This combination of theoretical and experimental accessibility screening offers the possibility of benefiting from the obvious advantages of both methods.

ACKNOWLEDGEMENTS

We thank the Deutsche Forschungsgemeinschaft for financial support and members of A3D GmbH-Antisense Design and Drug Development for helpful advice. A part of this work was supported by NIH grant AI29329 to J.J.R.

REFERENCES

1. Wagner,R.W. (1994) *Nature*, **372**, 333–335.
2. Stein,C.A. and Cheng,Y.-C. (1993) *Science*, **261**, 1004–1012.
3. Gewirtz,A.M. and Ratajczak,M.Z. (1998) In Stein,C.A. and Krieg,A.M. (eds), *Applied Antisense Oligonucleotide Technology*. Wiley-Liss, New York, NY, pp. 299–315.
4. Rossi,J.J. (1995) *Trends Biotechnol.*, **13**, 301–306.
5. Sczakiel,G. and Nedbal,W. (1995) *Trends Microbiol.*, **3**, 213–217.
6. Scherr,M., Grez,M., Ganser,A. and Engels,J.W. (1997) *J. Biol. Chem.*, **272**, 14304–14313.
7. Eckstein,F., Aurup,H., Benseler,F., Heidenreich,O., Marschall,P., Ng,M., Thomson,J. and Tuschl,T. (1993) *Nucleic Acids Symp. Ser.*, **29**, 115.
8. Patzel,V. and Sczakiel,G. (1998) *Nature Biotechnol.*, **16**, 64–68.
9. Peyman,A., Helsberg,M., Kretzschmar,G., Mag,M., Grabley,S. and Uhlmann,E. (1995) *Biol. Chem. Hoppe-Seyler*, **376**, 195–198.
10. Monia,B.P, Johnston,J.F., Geiger,T., Müller,M. and Fabro,D. (1996) *Nature Med.*, **2**, 668–675.
11. Scherr,M. and Rossi,J.J. (1998) *Nucleic Acids Res.*, **26**, 5079–5085.
12. Lima,W.F., Brown-Driver,V., Fox,M., Hanecak,R. and Bruice,T.W. (1996) *J. Biol. Chem.*, **272**, 626–638.
13. Milner,M., Mir,K.U. and Southern,E.M. (1997) *Nature Biotechnol.*, **15**, 537–541.
14. Matveeva,O., Felden,B., Audlin,S., Gesteland,R.F. and Atkins,J.F. (1997) *Nucleic Acids Res.*, **25**, 5010–5016.
15. Ho,S.P., Bao,Y.B., Lesher,T., Malhotra,R., Ma,L.Y., Fluharty,S.J. and Sakai,R.R. (1998) *Nature Biotechnol.*, **16**, 59–63.
16. Birikh,K.R., Berlin,Y.A., Soreq,H. and Eckstein,F. (1997) *RNA*, **3**, 429–437.
17. Lieber,A. and Strauss,M. (1995) *Mol. Cell. Biol.*, **15**, 540–551.
18. Tsuchihashi,Z., Khosla,M. and Herschlag,D. (1993) *Science*, **267**, 99–102.
19. Bertrand,E. and Rossi,J.J. (1994) *EMBO J.*, **13**, 213–221.
20. Homann,M., Nedbal,W. and Sczakiel,G. (1996) *Nucleic Acids Res.*, **24**, 4395–4400.
21. Nedbal,W., Frey,M., Willemann,B., Zentgraf,H.-W. and Sczakiel,G. (1997) *J. Mol. Biol.*, **266**, 677–687.
22. Patzel,V., Steidl,U., Kronenwett,R., Haas,R. and Sczakiel,G. (1999) *Nucleic Acids Res.*, **27**, 4328–4334.
23. Jost,J.P. and Saluz,H.P. (1993) In Jost,J.P. and Saluz,H.P. (eds), *DNA-Methylation: Molecular Biology and Biological Significance*. Birkhäuser Verlag, Boston, MA, pp. 356–384.
24. Wetmur,J.G. and Davidson,N. (1968) *J. Mol. Biol.*, **31**, 349–370.
25. Subirana,J.A. and Doty,P. (1966) *Biopolymers*, **4**, 171–187.